

## **Supplemental Information**

### **Age-dependent instability of mature neuronal fate in induced neurons from Alzheimer's patients**

**Jerome Mertens, Joseph R. Herdy, Larissa Traxler, Simon T. Schafer, Johannes C.M. Schlachetzki, Lena Böhnke, Dylan A. Reid, Hyungjun Lee, Dina Zangwill, Diana P. Fernandes, Ravi K. Agarwal, Raffaella Lucciola, Lucia Zhou-Yang, Lukas Karbacher, Frank Edenhofer, Shani Stern, Steve Horvath, Apua C.M. Paquola, Christopher K. Glass, Shauna H. Yuan, Manching Ku, Attila Szücs, Lawrence S.B. Goldstein, Douglas Galasko, and Fred H. Gage**

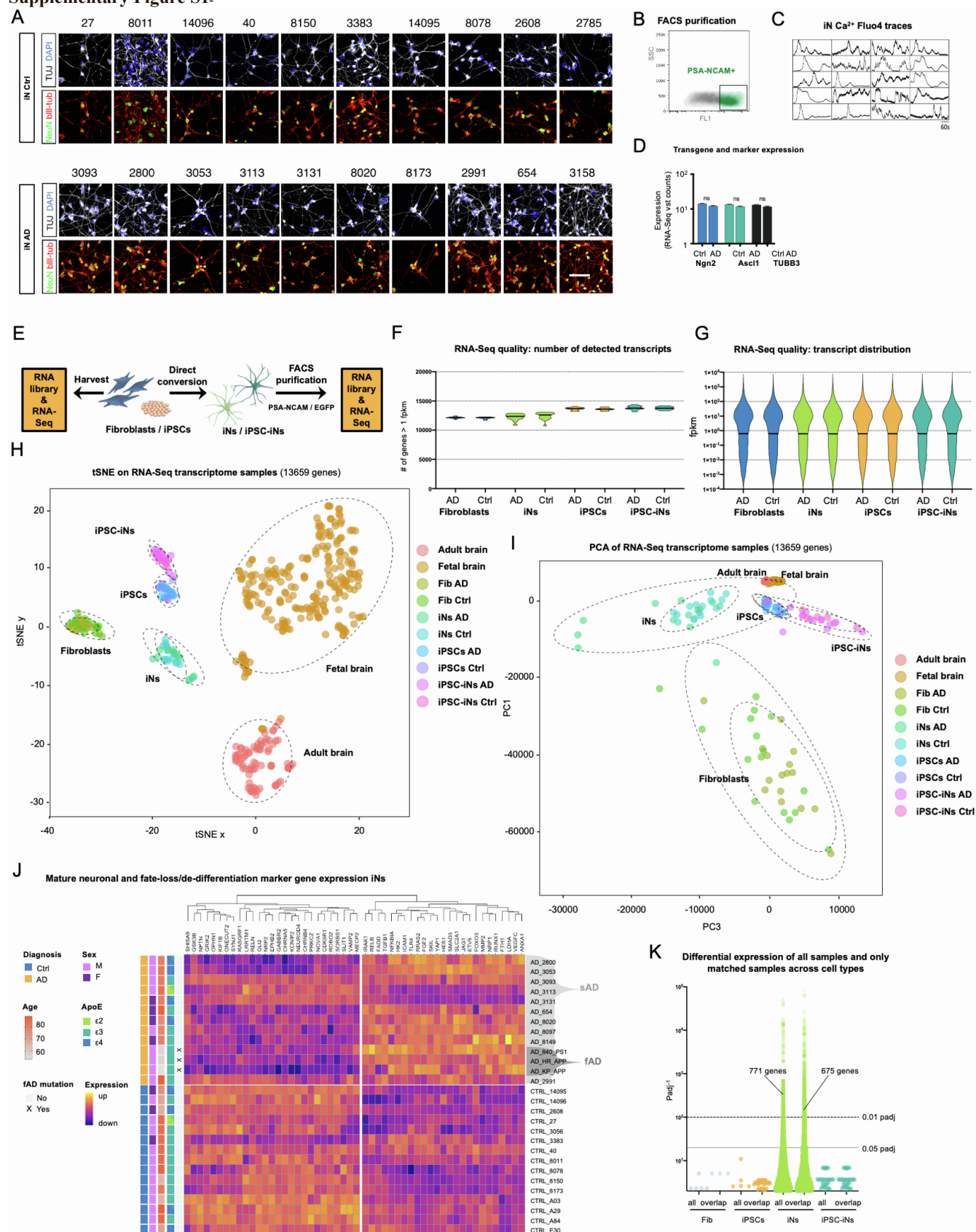
# Age-dependent instability of mature neuronal fate in induced neurons from Alzheimer’s patients

Mertens et al.

**SUPPLEMENTARY INVENTORY**

Supplementary Figure S1 .....	page 2
Supplementary Figure S2 .....	page 4
Supplementary Figure S3 .....	page 6
Supplementary Figure S4 .....	page 8
Supplementary Figure S5 .....	page 10
Supplementary Figure S6 .....	page 12
Supplementary Figure S7 .....	page 14
Supplementary Table 1 .....	page 15
Supplementary Table 2 .....	page 16
Supplementary Table 3 .....	in separate file
Supplementary Table 4 .....	in separate file
Supplementary Table 5 .....	page 17
Supplementary Table 6 .....	in separate file
Supplementary Table 7 .....	page 20

## Supplementary Figure S1.



**Supplementary Figure 1. Conversion of human fibroblasts into iNs, and whole-genome mRNA-Seq analysis and AD-specific DE analysis of donor fibroblasts, iNs, iPSCs and iPSC-iNs. Related to Fig.1.**

**A:** Representative immunofluorescent images of iNs from 20 individual donors labeled with DAPI,  $\beta$ III-tub (TUJ), and NeuN. Scale bar, 100  $\mu$ m.

**B:** FACS gating for the isolation of PSA-NCAM<sup>+</sup> (box) iNs following 3 weeks of conversion.

**C:** Line plots of live-cell imaging fluorescence intensity of Fluo-4 Ca<sup>2+</sup> transients in 20 individuals iN cells (n=4, 2 control and 2 AD subjects) reveals spontaneous network activity of iNs. Boxes, individual ROIs/cells.

**D:** Similar expression levels (vst-normalized counts) of Ngn2 and Ascl1 transgenes in Ctrl and AD iNs, and levels of pan-neuronal marker gene TUBB3 ( $\beta$ III-tub). Bars, mean $\pm$ SEM; ns, FDR<0.05 (DESeq2).

**E:** Workflow for generation of mRNA-Seq transcriptome profiles from fibroblasts and iPSCs, and FACS-purified mRNA-Seq from iNs and iPSC-iNs following 3 weeks of conversion.

**F:** Violin plot showing deepness/quality of mRNA-Seq data from all 103 samples represented as the number of mapped reads with >1 fragments per kilobase of transcript per million (fpkm) per Ctrl and AD group. All samples show a high level of transcript detection and no apparent differences between control and AD samples are noted.

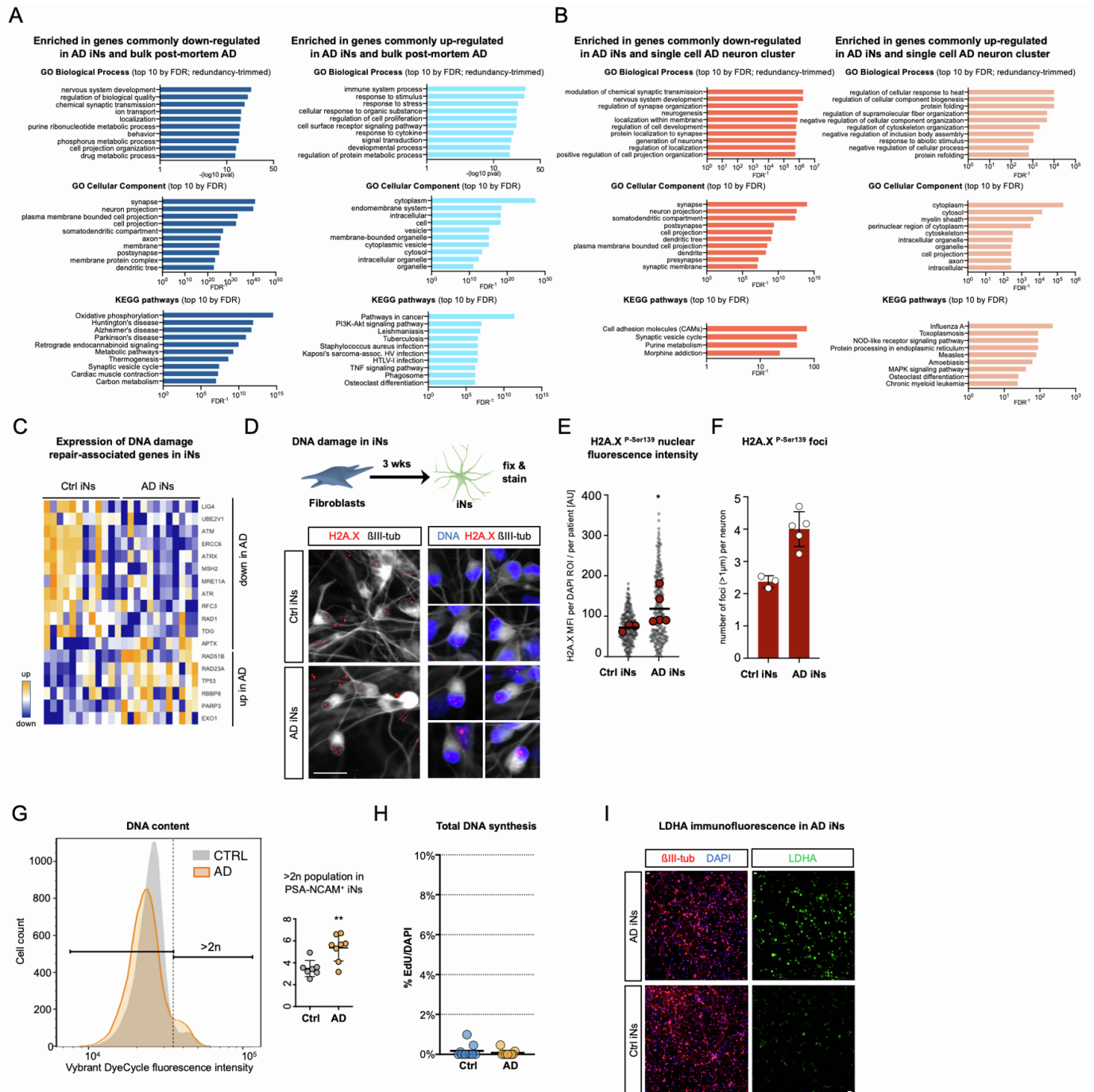
**G:** Violin plot for transcript distribution (fpkm) within each Ctrl and AD group indicates similar transcription level distribution between Ctrl and AD, and between all four cell types.

**H-I:** t-distributed stochastic neighbor embedding (tSNE, **H**) and principal component analysis (PCA, **I**) plots of mRNA-Seq data from fibroblasts (n=32), iNs (n=28), iPSCs (n=21), and iPSC-iNs (n=20), including all fetal (n=237) and adult (n=77) samples from the Allen BrainSpan RNA-Seq atlas. All 13,659 genes that were detected in our and the BrainSpan dataset were used for tSNE and PCA.

**J:** Heatmap based on vst-normalized counts depicting the mature neuronal and fate-loss/de-differentiation marker gene expression in control and AD iNs (sAD, sporadic AD; fAD, familial AD). All depicted marker genes are sorted via hierarchical clustering. All marker genes are both highly significant (padj<0.01) AD iN DE genes, and part of the key gene sets presented in Fig. 3C (mature neuronal gene sets) and Fig. 4D (fate-loss/de-differentiation gene sets).

**K:** Significant AD DE genes in all four cell types for the full set of samples (*all*), and for only those donors for which all four cell types are available (*overlap*, 8x Ctrl; 11x AD; with the exception of donor sample 3158 which is not available for iNs). This isogenic 'matched sample' analysis confirms significant AD DE gene expression only in iNs, but not in the other cell types.

## Supplementary Figure S2



**Supplementary Figure S2. Gene set enrichment analysis of overlapping AD genes between iNs and post mortem brain, and DNA damage and aneuploidy assessment in AD iNs. Related to Fig.2 and Fig.5.**

**A:** Gene set enrichment analyses of down-regulated (left, dark blue) and up-regulated (right, light blue) genes that are commonly changed in the same direction in AD iNs and post mortem data sets (pooled genes from Fig. 2D). Bar graphs show all top 10 (by FDR) gene sets for each GSEA category (GO PB, GO CC, and KEGG).

**B:** Gene set enrichment analyses of down-regulated (left, dark orange) and up-regulated (right, light orange) genes that are commonly changed in the same direction in AD iNs and post mortem snRNA-Seq neurons (Grubman et al., 2019). Bar graphs show all top 10 (by FDR) gene sets for each GSEA category (GO PB, GO CC, and KEGG).

**C:** Heatmap based on vst-normalized counts depicting DNA damage repair-associated gene expression in control and AD iNs.

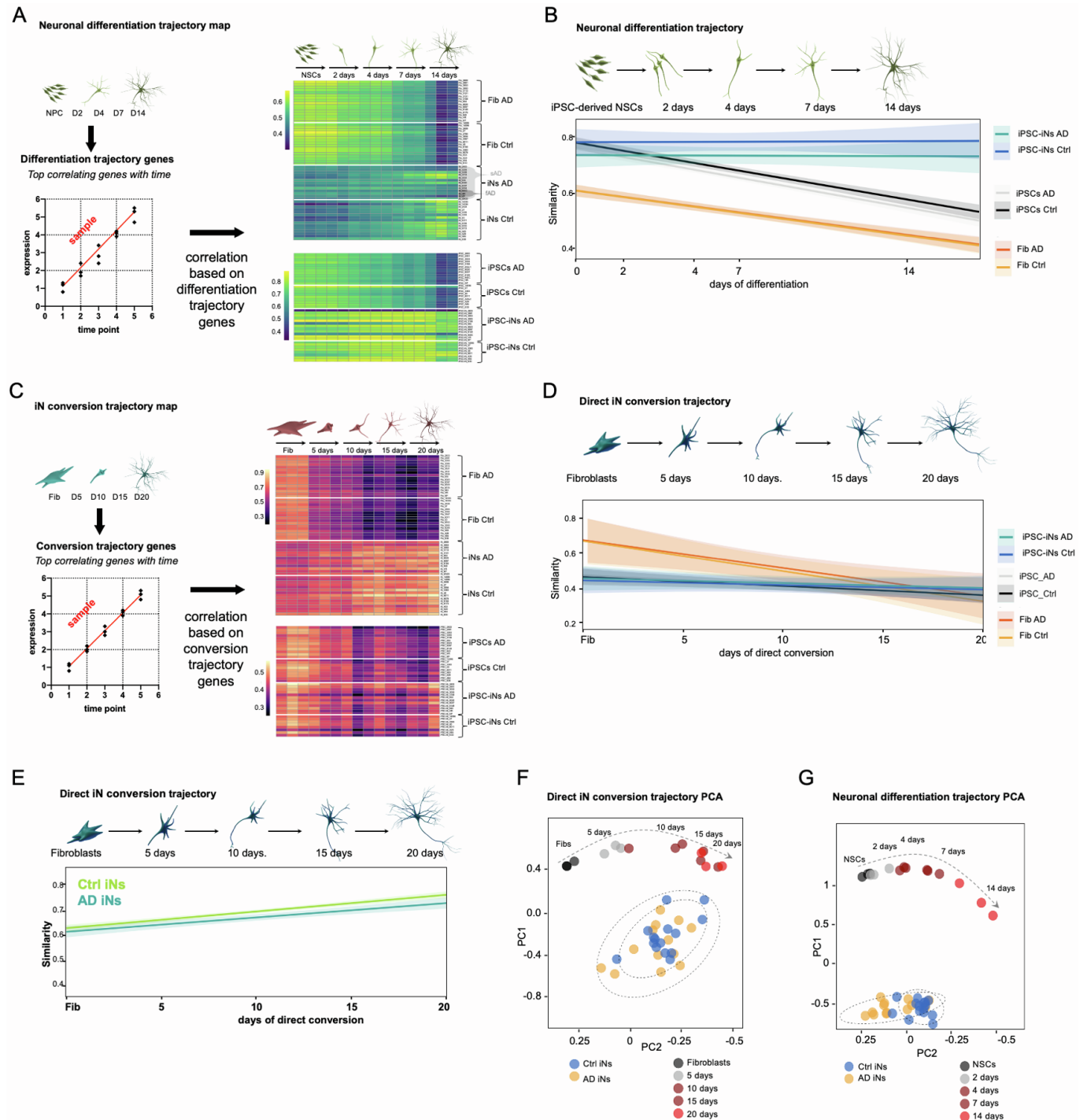
**D-F:** For the assessment of DNA damage levels, immunofluorescence analysis for H2A.X-pSer139 was performed following 3 weeks of conversion. Representative Immunofluorescence images show intensity and distribution of H2A.X-pSer139 immunoreactivity in iNs (**D**). Mean fluorescence intensities (MFI) of nuclear DAPI-colocalized H2A.X-pSer139 immunofluorescence intensity (**E**; gray circles, nuclei; red circles, subjects), and numbers of H2A.X-pSer139-positive foci (**F**; white circles, subjects) were quantified. Bars, mean $\pm$ SD; subjects, control (n=3); AD (n=5); unpaired t-test; scale bar, 100  $\mu$ m. unpaired t-test based on subjects, \*p<0.05.

**G:** DNA content of live control (n=7) and AD (n=8) iNs was measured following 3 weeks of conversion using the cell-permeable DNA marker Vybrant DyeCycle. FACS histogram shows merged averages of all tested control and AD iNs (left), and scatter plot shows fractions of cells with >2n DNA content for each individual (right). Bars, mean $\pm$ SD; unpaired t-test.

**H:** Quantification of control (n=9) and AD (n=9) iNs fluorescently labeled for DNA replication following 3 weeks of iN conversion and 72h of EdU exposure. EdU incorporation was only rarely observed in  $\beta$ III-tub<sup>-negative</sup> fibroblasts, and never in  $\beta$ III-tub<sup>+</sup> neurons (Fig. 5F). Circles, subjects.

**I:** Representative low-magnification immunofluorescence images of iNs for  $\beta$ III-tub and LDHA. Scale bars, 20  $\mu$ m.

## Supplementary Figure S3



Supplementary Figure S3. Mapping of iN transcriptomes to the neuronal differentiation trajectory, and the direct iN conversion trajectory. Related to Fig.4.

**A:** Genes with the strongest linear regression with the differentiation timeline of iPSC-derived neural stem cells (365 genes;  $r^2 > 0.8$ , ) were used as differentiation trajectory genes. Pearson correlation based on differentiation trajectory genes was performed to compare all fibroblast, iN, iPSC, and iPSC-iN transcriptome samples to the five time points of neuronal differentiation (0, 2, 4, 7, and 14 days), displayed as a heatmap for all individual samples.

**B:** Similarity of fibroblasts, iPSCs, and iPSC-iNs (each separated into control and AD) to the neuronal differentiation trajectory from longitudinal mRNA-Seq data of iPSC-derived neural stem cells differentiation into neurons.

**C:** Genes with the strongest linear regression with the direct iN conversion timeline of fibroblasts into iNs (47 genes;  $r^2 > 0.9$ , (Herdy et al., 2019)) were used as conversion trajectory genes. Pearson correlation based on conversion trajectory genes was performed to compare all fibroblast, iN, iPSC, and iPSC-iN transcriptome samples to the five time points of neuronal conversion (0, 5, 10, 15, and 20 days), displayed as a heatmap for all individual samples.

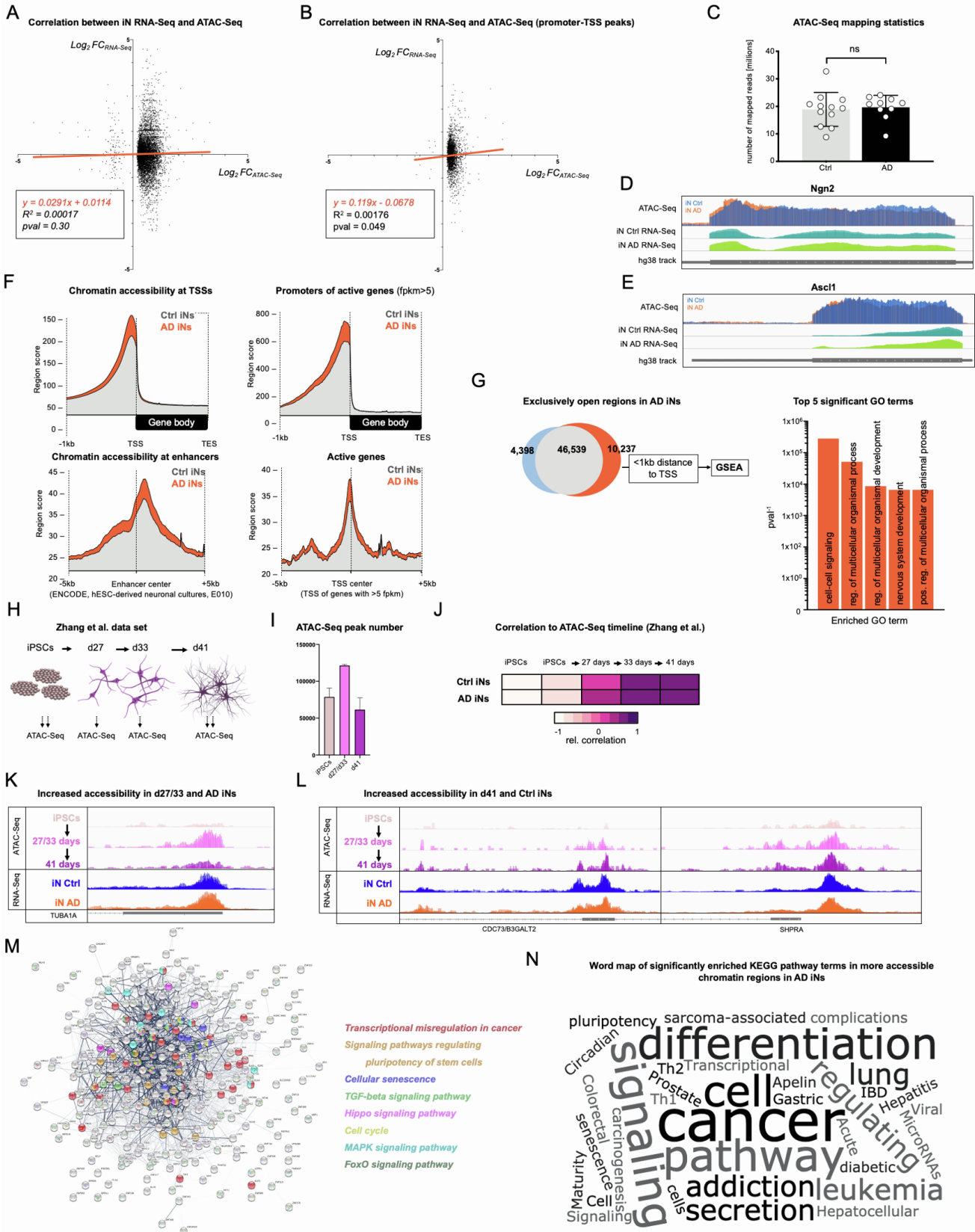
**D-E:** Similarity of control and AD fibroblasts, iPSCs, and iPSC-iNs (**D**), and control and AD iNs (**E**) to the direct iN conversion trajectory from longitudinal mRNA-Seq data of fibroblast-to-iN conversion. Trajectory genes listed in Supplementary Table 4.

**F:** PCA based on neuronal differentiation trajectory genes, for the original differentiation trajectory samples (n=3 per time point;), and control and AD iNs.

**G:** PCA based on neuronal conversion trajectory genes, for the original differentiation trajectory samples (n=3 per time point; (Herdy et al., 2019)), and control and AD iNs.



Supplementary Figure S4



**Supplementary Figure S4. ATAC-Seq analysis of AD iNs, correlation with RNA-Seq, and mapping of the AD iN chromatin landscape to profiles from iPSC-based neuronal differentiation. Related to Fig.6.**

**A-B:** Correlation of Ctrl versus AD iN differential ATAC peak fold changes with differential RNA-Seq expression fold changes. Global (all genomic annotations) chromatin accessibility and gene expression show a positive correlation trend on a gene-by-gene basis (**A**), and promoter-TSS chromatin accessibility significantly correlated with gene expression (**B**).

**C:** No differences in the number of uniquely mapped reads between Ctrl and AD iNs (unpaired t-test). Bars, mean $\pm$ SD.

**D-E:** ATAC-Seq and RNA-Seq tracks for Ngn2 (**D**) and Ascl1 (**E**) transgenes in merged Ctrl and AD iNs indicate no differences between Ctrl and AD iNs in proviral transgene integration and expression.

**F:** Density plot of differential accessibility ATAC-Seq peaks separated by annotation, including TSS, over peak fold change (Ctrl versus AD iNs).

**G:** Chromatin accessibility region scores at ATAC peak regions at all known TSSs (upper left panel), at promoters of active (>5fpm in RNA-Seq) genes (upper right panel), centered around TSS ( $\pm$ 5kb) of neuronal enhancers (ENCODE E010 data set; lower left panel), and centered around the TSSs of active (>5fpm in RNA-Seq) genes. Bar graph shows the top 5 significantly enriched GO terms of promoter-associated peaks exclusively open in AD iNs, but that do not intersect with called peaks in Ctrl iNs. Bars, significance  $pval^{-1}$ .

**H:** Schematic summarizing the data we used from Zhang et al. (Zhang et al., 2018), which performed ATAC-Seq from iPSCs, and iPSC-derived neural cultures from 27, 33 and 41 days of differentiation.

**I:** Significantly more open chromatin regions (peaks) were detected in the more immature 27-day and 33-day cultures, compared to the 41-day and iPSC time points. Bars, mean $\pm$ SD.

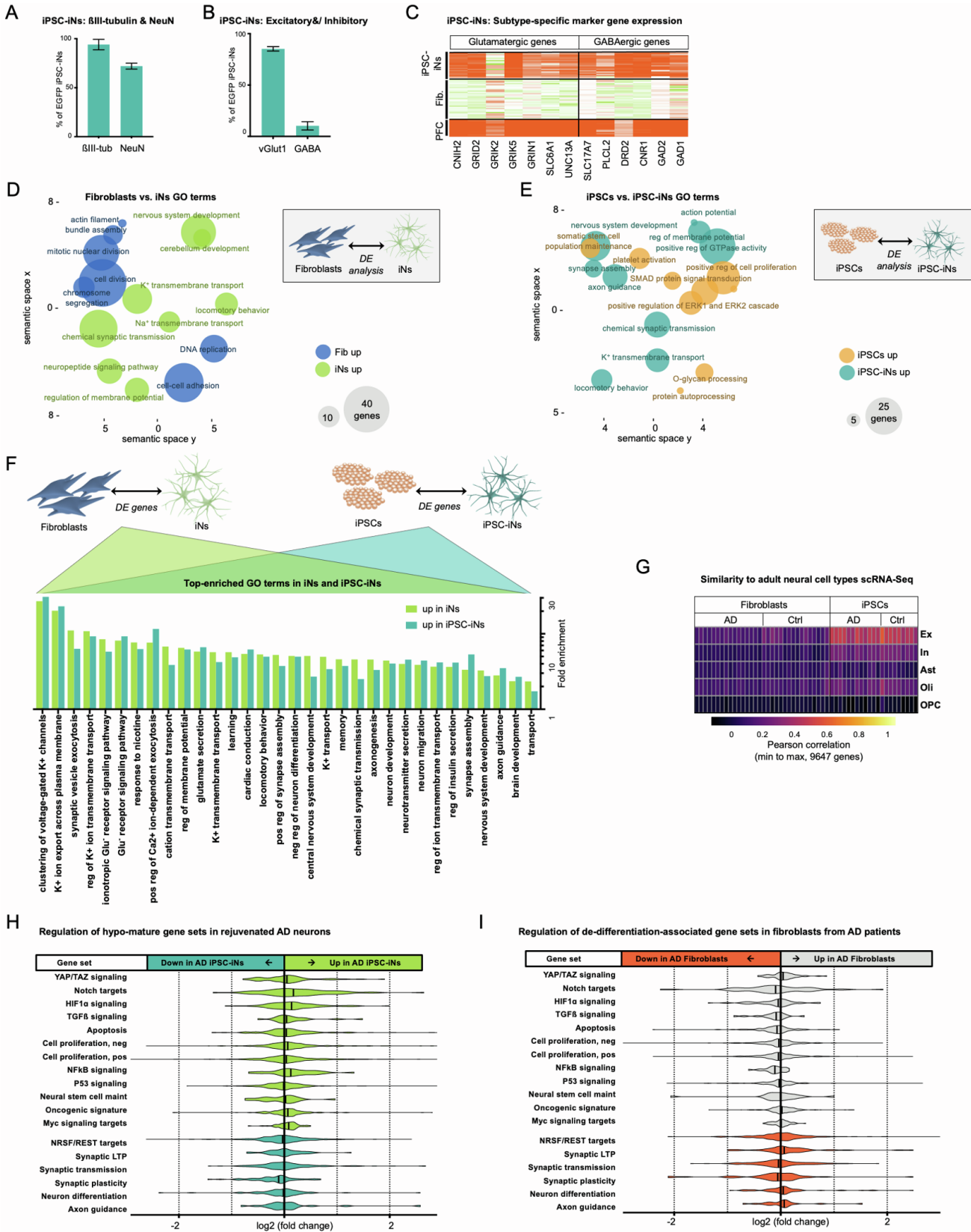
**J:** Heatmap showing the higher relative correlation of AD iNs to the less-differentiated 27-days time point, based on relative Pearson correlation values of the global bedgraph peak profiles of our Ctrl and AD iNs to the differentiation time line.

**K-L:** ATAC-Seq tracks of TUBA1A (**K**), a representative gene that shows transient increased accessibility in immature iPSC-neurons and in AD iNs; and tracks of CDC73 and SHRPA (**L**), as representative genes showing a steady increase in accessibility with mature, and lower accessibility in AD iNs than in Ctrl iNs.

**M:** STRING network showing KEGG pathway GSEA of DNA-binding factors that are enriched in chromatin regions differentially accessible in AD iNs. Enriched KEGG pathways that directly relate to cancer-like cellular transformation, senescence, and RNA-Seq gene sets are color-coded in the interaction network, which shows all significant DNA-binding factors detected in our motif analysis.

**N:** Word cloud (wordclouds.com) of significantly enriched KEGG pathways in motif binding factors.

Supplementary Figure S5



**Supplementary Figure S5. Comparison of iNs and iPSC-iNs by DE analysis and gene set enrichment analyses. Related to Fig.7.**

**A:** Quantification of NeuN,  $\beta$ III-tubulin (A), vGlut1 and GABA-positive (B) immunocytochemistry in FACS-purified iPSC-iN cultures. Bars, mean $\pm$ SD.

**B:** Quantification of immunofluorescence images for vGlut1 and GABA-positive iPSC-iN cultures. Bars, mean $\pm$ SD.

**C:** Expression levels of glutamatergic and GABAergic neuron marker genes in iPSC-iNs compared to fibroblasts and prefrontal cortex (PFC) samples. Green: low; red: high expression.

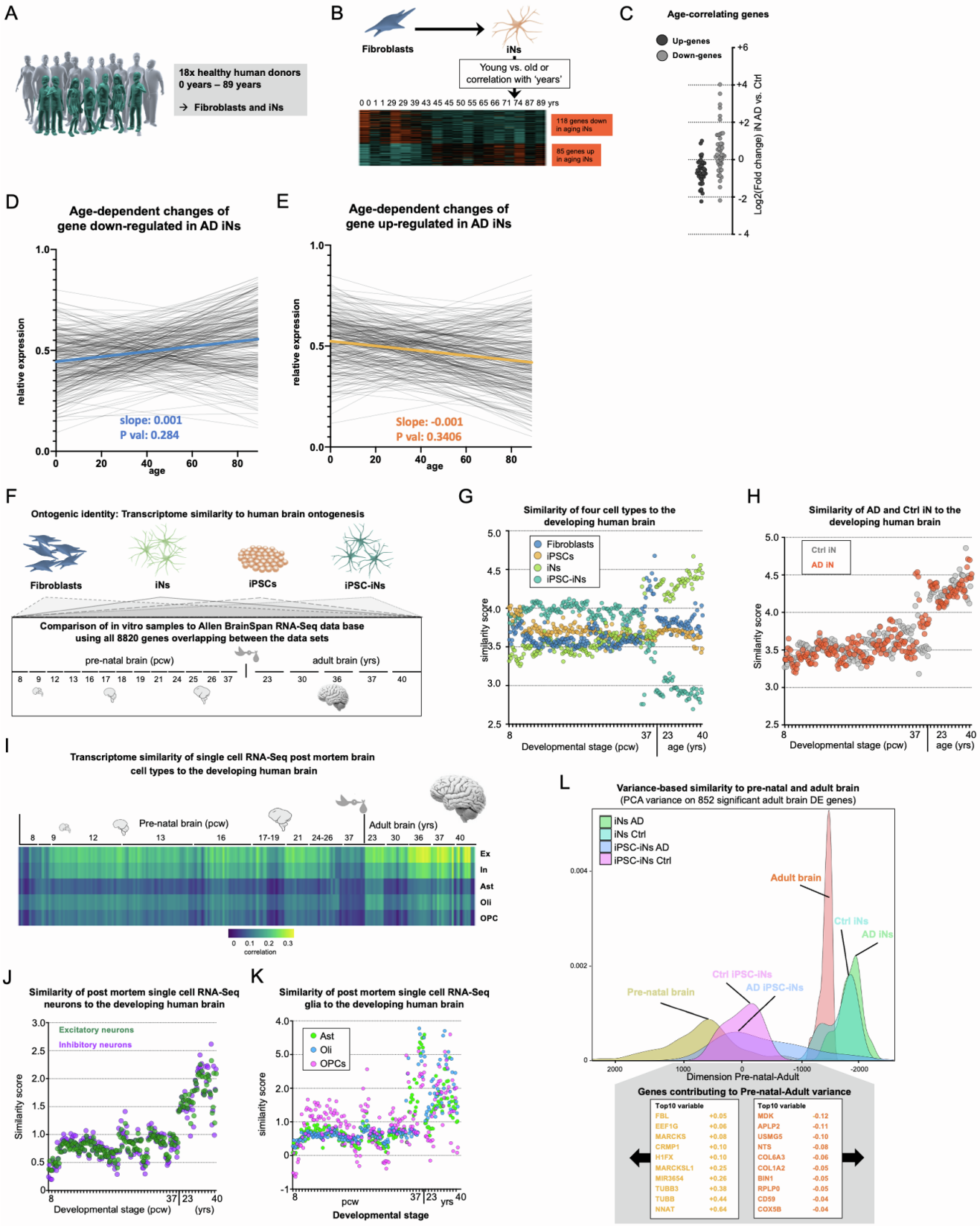
**D-E:** Mapping of redundancy-trimmed GSEA in semantic REVIGO space. Enriched GO BP terms in significant DE genes between fibroblasts (blue) and iNs (green)(D); and significant DE genes between iPSCs (orange) and iPSC-iNs (petrol)(E). Size of circles corresponds to number of input genes per GO term.

**F:** Comparison of fold enrichment of neural GO BP terms upregulated both between iNs and fibroblasts, and between iPSC-iNs and iPSCs.

**G:** Heatmap showing transcriptome-wide Pearson correlation between iNs and iPSC-iNs and adult human cortex-derived excitatory neurons (Ex), inhibitory (In), astrocytes (Ast), oligodendrocytes (Oli), and oligodendrocyte precursor cells (OPC; from single-nucleus-RNA-Seq data, (Mathys et al., 2019)). All 9,647 genes overlapping between our data, the single-nucleus-RNA-Seq data and BrainSpan datasets were used for the correlation analysis in R).

**H-I:** Violin plots showing gene expression changes between control and AD fibroblasts (H) and iPSC-iNs (I) of selected gene sets also presented in Fig. 3C (mature neuronal gene sets) and Fig. 4D (fate-loss/de-differentiation gene sets) for control and AD iNs. No significant differential expressed genes or any apparent differential regulation of any of these pathways was detected in fibroblasts or iPSC-iNs. The data shown in this plot were used for the paired non-parametric t-tests of the control versus AD log2 fold changes observed iNs to calculate significance over potential donor- and cell-type biases (see Fig. 3C and Fig. 4D).

Supplementary Figure S6



**Supplementary Figure S6. Age-dependent gene expression in Ctrl and AD iNs, and similarity of fibroblasts, iNs, iPSCs and iPSC-iNs to human brain development stages. Related to Fig.7.**

**A:** Schematic depicting cohort of 18 healthy human donors ranging from newborns to 89 years of age from which iNs were generated and subjected to mRNA-Seq (Mertens et al., 2015).

**B:** Differential expression analysis reveals 118 down-regulated and 85 up-regulated aging genes used for the assessment of age-regulated transcriptional changes in AD iNs (Fig. 7J).

**C:** Expression of genes correlating  $|\text{Cor}| > 0.6$  with donor age (Mertens et al., 2015) in control versus AD iNs. Genes that correlate positively with subject age shown in dark gray, negatively correlating genes shown in light gray. Positive values indicate up-regulation in AD iNs over Ctrl. Genes that positively correlate with age in healthy aging appear slightly down-regulated in AD iNs. Each dot represents one gene.

**D-E:** Relative age-dependent expression trend of AD iN up-regulated (**D**) and AD iN down-regulated (**E**) genes in the healthy aging iN cohort. The analysis shows no significant correlation, but a slight inverse trend, with genes down-regulated in AD positively correlating with age and genes up-regulated in AD negatively correlating with age (**E**).

**F:** Ontogenic neural identity was assessed by transcriptional similarity of our 4 cell types to post mortem human brain RNA-Seq data (BrainSpan, n=215 cortical samples).

**G-H:** Normalized transcriptome similarity scores for fibroblast, iNs, iPSCs, and iPSC-iNs (**G**), and for control and AD iNs (**H**) with the 215 cortical samples from BrainSpan (163 fetal and 52 adult samples).

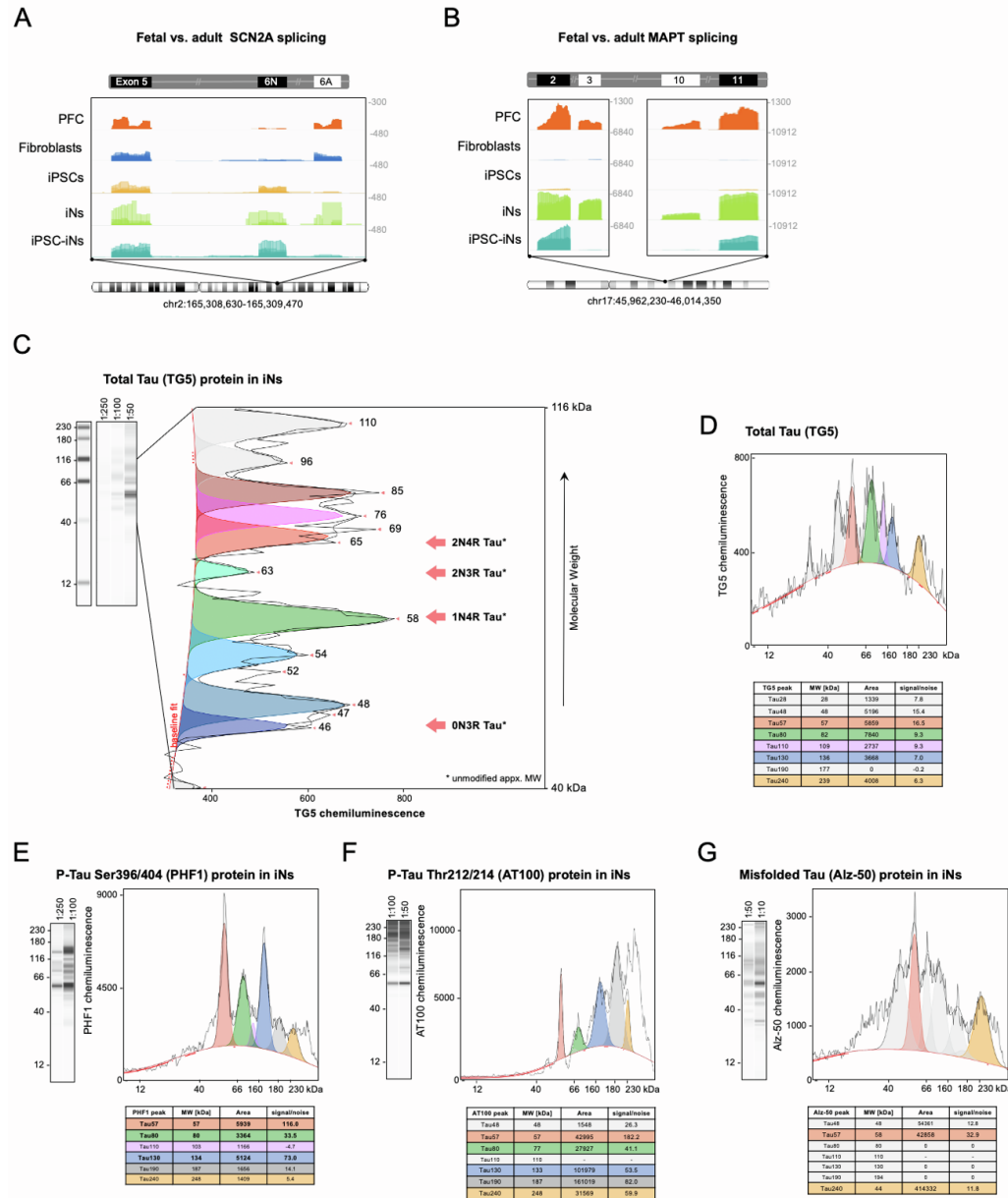
**I:** Heatmap showing transcriptome-wide correlation of adult human cortex-derived excitatory neurons (Ex), neurons (In), astrocytes (Ast), oligodendrocytes (Oli), and oligodendrocyte precursor cells (OPC; from single-nucleus-RNA-Seq data (Mathys et al., 2019) to cortical samples (n=215) of the Allen BrainSpan data set. All 9,647 genes overlapping between our data, the single-nucleus-RNA-Seq data, and the BrainSpan data sets were used for correlation.

**J-K:** Normalized transcriptome similarity scores for adult human cortex-derived excitatory neurons (Ex) and inhibitory neurons (In) (**D**), and glial cell types (**E**) astrocytes (Ast), oligodendrocytes (Oli), oligodendrocyte precursor cells (OPC; from single-nucleus-RNA-Seq data (Mathys et al., 2019) with the 163 fetal developmental and 52 adult cortical BrainSpan samples.

**L:** Density plot showing the localizations of control and AD iN (n=28), iPSC-iN (n=20) samples, and BrainSpan pre-natal (n=163) and adult (n=52) cortical samples along pre-natal-adult variance dimension. Pre-natal-adult variance is based on PCA of 852 genes overrepresented in adult samples over fetal samples of BrainSpan transcriptome atlas and separates fetal from adult brain samples, and iN and iPSC-iN co-localize with adult and fetal samples, respectively. Boxes below show the top 10 genes with the highest positive and negative loadings in the Pre-natal-adult principal component.



## Supplementary Figure S7



## Supplementary Figure S7. Adult-like splicing patterns and MAPT protein variants in iNs. Related to Fig.7.

**A-B:** Genome browser tracks of mRNA-Seq data from merged fibroblasts, iNs, iPSCs and iPSC-iNs and around the fetal (6N) and adult (6A) exon of the SCN2A gene (**A**), and of the adult-specific spliced exons 3 and 10 of the MAPT gene (**B**). Scale values on right y-axis represent number of aligned reads per cell type. PFC, post mortem pre-frontal cortex samples (Mertens et al., 2015).

**C-D:** Capillary Western blot (ProteinSimple) analysis for total-Tau (TG5 antibody) shows a wide distribution of Tau species in iNs. The pseudo-gel (**C**; left) and electropherogram (**C**; main box) views show different Tau species, including variants at 65 kDa and over, which correspond to the size of the 2N4R isoform and modified version of it. TG5 electropherogram also shows larger peaks up to 230 kDa (**D**).

**E-G:** Capillary Western blot analysis for phosho-Tau (PHF1, pSer396/404 (**E**); AT100, pThr212/214 (**F**); and Alz-50, misfolded Tau (**G**) antibodies). The pseudo-gel (left) and electropherogram (main boxes) views show that the antibodies detect different Tau species, with different affinities to different species, but also many of the same peaks were detected. Coloring of peaks is used to make the same peaks recognizable throughout the figure, and the tables (bottom) list molecular weights (MW), signal strength (area under the curve), and signal-to-noise ratios (S/N >20 typically considered significant) for each peak following background fit (red line).

**Supplementary Table S1**

Table of all human fibroblast samples used in this study. Related to Fig.1.

ID	Group	fAD mutation	Age (of biopsy)	Gender	Clinical Dx	Dx data	APOE
A84	control	no	87	M	non-demented	Clinical summary report	3...3
A29	control	no	89	M	non-demented	Clinical summary report	3...4
A03	control	no	66	M	non-demented	Clinical summary report	3...3
27	control	no	86	M	non-demented	ADRC study participant	2...3
8011	control	no	85	M	non-demented	ADRC study participant	3...3
14096	control	no	69	M	non-demented	ADRC study participant	3...3
40	control	no	84	M	non-demented	ADRC study participant	3...3
2785	control	no	78	F	non-demented	ADRC study participant	3...4
8150	control	no	65	M	non-demented	ADRC study participant	3...3
3383	control	no	84	F	non-demented	ADRC study participant	3...3
3056	control	no	85	M	non-demented	ADRC study participant	3...3
14095	control	no	75	F	non-demented	ADRC study participant	3...4
E30	control	no	71	M	non-demented	Clinical summary report	4...4
8072	control	no	76	F	non-demented	ADRC study participant	3...4
8078	control	no	87	M	non-demented	ADRC study participant	3...3
8094	control	no	82	M	non-demented	ADRC study participant	3...4
3367	control	no	79	M	non-demented	ADRC study participant	2...3
2608	control	no	67	F	non-demented	ADRC study participant	4...4
8173	control	no	81	M	non-demented	ADRC study participant	3...3
8149	AD	no	79	F	demented, prob. AD	ADRC study participant	3...3
3093	AD	no	81	M	demented, prob. AD	ADRC study participant	3...3
2991	AD	no	89	M	demented, prob. AD	ADRC study participant	3...3
8097	AD	no	78	M	demented, prob. AD	ADRC study participant	3...3
2800	AD	no	80	M	demented, prob. AD	ADRC study participant	3...4
654	AD	no	88	F	demented, prob. AD	ADRC study participant	3...3
3053	AD	no	82	M	demented, prob. AD	ADRC study participant	4...4
3113	AD	no	83	M	demented, prob. AD	ADRC study participant	2...3
3131	AD	no	80	F	demented, prob. AD	ADRC study participant	3...4
8020	AD	no	76	F	demented, prob. AD	ADRC study participant	3...4
8175	AD	no	83	M	demented, prob. AD	ADRC study participant	3...3
3158	AD	no	75	F	demented, prob. AD	ADRC study participant	3...3
3121	AD	no	75	F	demented, prob. AD	ADRC study participant	3...3
KP	AD	APPSWE	53	M	familial AD	Clinical summary report	3...3
HR	AD	APPV717F	57	M	familial AD	Clinical summary report	3...3
840C	AD	PS1A246E	56	M	familial AD	Clinical summary report	3...3
Hans	AD	PS1 mut	41	M	familial AD	Clinical summary report	
A54	young	no	29	M	non-demented	Clinical summary report	
E1	young	no	29	F	non-demented	Clinical summary report	
E4	young	no	43	M	non-demented	Clinical summary report	

**Clinical follow-up of sporadic AD subjects (available only for ADRC participants):**

Autopsy of the following subjects confirmed classical AD pathology (amyloid plaques Thal stage 5 and/or extensive neuritic plaques, and Braak stage 6 neurofibrillary tau pathology): 8149, 3093, 8097, 8020, 8175, and 3158.

Autopsy for subject 654 confirmed AD with amyloid, but died at a stage of moderate dementia with Braak stage 3 tau pathology.

Autopsy for subjects 2800, 3113, 2991 and 3121 showed hippocampal atrophy with signs for hippocampal sclerosis and TDP43 inclusions, and only partially showed significant amyloid or tau pathology. These AD cases thus had neurodegenerative co-morbidities and can be classified as non-classical AD cases that clinically mimicked classical AD.

No autopsy was performed for subject 3131. Three years of follow-up showed clinical progression with severe memory loss, worsening of other cognitive domains, and severe dementia. CSF biomarkers showed low A-beta42, high tau and high P-tau, consistent with AD. MRI showed hippocampal atrophy, and hippocampal sclerosis co-morbidity remains possible.

No autopsy was performed for subject 3053. Eight years of follow-up showed clinical progression with severe memory loss, worsening of other cognitive domains, and severe dementia. MRI showed hippocampal atrophy, consistent with AD.



Supplementary Table S2

Table of control and AD subjects assessed in this study for each experiment. Related to all Figures.

ID	Group	RNA-Seq				DNAm EPIC		ATAC-Seq			
		Fib	IN	IPSC	IPSC-IN	Fib	IN	Fib	IN	IN	IN
A84	control	X	X	X	X					X	X
A29	control	X	X	X	X					X	X
A03	control	X	X	X	X						
27	control	X	X	X	X					X	X
8011	control	X	X	X	X	X	X	X	X		
14096	control	X	X	X	X					X	X
40	control	X	X	X	X					X	X
2785	control	X	X	X	X	X	X	X	X	X	X
8150	control	X	X	X	X	X	X	X	X	X	X
3383	control	X	X	X	X						
3056	control	X	X	X	X						
14095	control	X	X	X	X	X	X	X	X	X	X
E30	control	X	X	X	X	X	X	X	X	X	X
8072	control										
8078	control	X	X			X	X			X	X
8094	control					X	X				
3367	control	X	X			X	X				
2608	control	X	X							X	X
8173	control	X	X							X	X
8149	AD	X	X	X	X	X	X	X	X		
3093	AD	X	X	X	X	X	X			X	X
2991	AD	X	X	X	X						
8097	AD	X	X	X	X					X	X
2800	AD	X	X	X	X					X	X
654	AD	X	X	X	X	X	X			X	X
3053	AD	X	X	X	X	X	X	X	X	X	X
3113	AD	X	X	X	X	X	X	X	X	X	X
3131	AD	X	X			X	X	X	X	X	X
8020	AD	X	X	X	X	X	X	X	X	X	X
8175	AD	X	X							X	X
3158	AD	X	X	X	X	X	X	X	X	X	X
3121	AD	X	X	X	X	X	X			X	X
KP	AD	X	X	X	X						
HR	AD	X	X	X	X					X	X
840C	AD	X	X	X	X						
Hans	AD										
A54	young	*	*	*	*						
E1	young	*	*	*	*						
E4	young	*	*	*	*						
n (Ctrl versus AD)		16 v 16	15 v 13	9 v 12	8 v 12	8 v 8	8 v 8	11 v 10			

\* assessed also in Mertens et al. Cell Stem Cell 2015

X assessed in this study

## Supplementary Table S5

Table of enriched GO terms in AD iNs. Related to Fig.3, Fig.4.

Enriched GO terms in down-regulated genes in AD iNs				Enriched GO terms in up-regulated genes in AD iNs			
Term	description	PValue	Fold Enrich.	Term	description	PValue	Fold Enrich.
GO:0006351	transcription, DNA-templated	8.72E-09	1.59	GO:0001666	response to hypoxia	6.95E-09	3.61
GO:0006355	regulation of transcription, DNA-templated	1.50E-08	1.68	GO:0055114	oxidation-reduction process	1.63E-07	2.10
GO:0043547	positive regulation of GTPase activity	2.07E-05	1.90	GO:0001525	angiogenesis	1.74E-07	2.98
GO:0048511	rhythmic process	3.14E-05	4.77	GO:0008285	negative regulation of cell proliferation	2.27E-07	2.38
GO:0051056	regulation of small GTPase mediated	4.89E-05	3.04	GO:0045766	positive regulation of angiogenesis	3.28E-07	3.91
GO:0035023	regulation of Rho protein signal	3.47E-04	3.45	GO:0022617	extracellular matrix disassembly	1.86E-06	4.51
GO:0061003	positive regulation of dendritic spine	4.37E-04	8.59	GO:0006954	inflammatory response	7.71E-06	2.20
GO:0007399	nervous system development	9.36E-04	2.02	GO:0007165	signal transduction	1.16E-05	1.60
GO:0007411	axon guidance	0.0012	2.43	GO:0030335	positive regulation of cell migration	1.60E-05	2.79
GO:0035556	intracellular signal transduction	0.0012	1.81	GO:0042060	wound healing	1.76E-05	4.02
GO:0007626	locomotory behavior	0.0017	3.07	GO:0045429	positive regulation of nitric oxide biosynthetic process	2.17E-05	5.48
GO:0006491	N-glycan processing	0.0019	6.44	GO:0007568	aging	2.82E-05	2.86
GO:0051965	positive regulation of synapse assembly	0.0022	3.46	GO:0008284	positive regulation of cell proliferation	3.46E-05	1.98
GO:0007420	brain development	0.0034	2.15	GO:0036327	cell adhesion mediated by integrin	3.51E-05	10.00
GO:0001764	neurite migration	0.0035	2.66	GO:0071549	cellular response to dexamethasone stimulus	3.86E-05	6.65
GO:0007158	neuron cell-cell adhesion	0.0054	6.71	GO:0008360	regulation of cell shape	9.04E-05	2.91
GO:0003222	ventricular trabecula myocardium	0.0054	6.71	GO:0043066	negative regulation of apoptotic process	9.07E-05	1.93
GO:0032012	regulation of ARF protein signal	0.0054	6.71	GO:0042493	response to drug	9.15E-05	2.18
GO:0060384	innervation	0.0084	5.96	GO:0050731	positive regulation of peptidyl-tyrosine phosphorylation	1.01E-04	3.66
GO:0007417	central nervous system development	0.0100	2.33	GO:0030198	extracellular matrix organization	1.25E-04	2.51
GO:0007018	microtubule-based movement	0.0127	2.65	GO:0036499	PERK-mediated unfolded protein response	1.31E-04	10.71
GO:0043065	positive regulation of apoptotic process	0.0134	1.72	GO:0030512	negative regulation of transforming growth factor beta receptor	1.63E-04	4.02
GO:0055117	regulation of cardiac muscle contraction	0.0148	5.11	GO:0030514	negative regulation of BMP signaling pathway	1.94E-04	4.76
GO:0010977	negative regulation of neuron projection	0.0155	3.42	GO:0001843	neural tube closure	2.19E-04	3.62
GO:0007156	homophilic cell adhesion via plasma	0.0161	2.54	GO:0003246	response to lipopolysaccharide	2.35E-04	2.61
GO:0000226	microtubule cytoskeleton organization	0.0170	2.72	GO:0001938	positive regulation of endothelial cell proliferation	3.24E-04	3.72
GO:0002027	regulation of heart rate	0.0173	3.90	GO:0071407	cellular response to organic cyclic compound	3.62E-04	3.99
GO:0030036	actin cytoskeleton organization	0.0181	2.15	GO:0030109	collagen fibril organization	3.66E-04	4.94
GO:0098735	positive regulation of the force of heart	0.0197	12.88	GO:0006564	L-serine biosynthetic process	3.90E-04	21.42
GO:1904885	beta-catenin destruction complex assembly	0.0197	12.88	GO:0031663	lipopolysaccharide-mediated signaling pathway	5.65E-04	5.35
GO:0090102	cochlea development	0.0235	4.47	GO:0045599	negative regulation of fat cell differentiation	6.21E-04	4.59
GO:0090314	positive regulation of protein targeting to	0.0235	4.47	GO:0070059	intrinsic apoptotic signaling pathway in response to endoplasmic	6.88E-04	5.19
GO:0007422	peripheral nervous system development	0.0235	4.47	GO:0030574	collagen catabolic process	7.07E-04	3.68
GO:0047496	vesicle transport along microtubule	0.0248	6.14	GO:0034142	tol-like receptor 4 signaling pathway	0.0011	7.14
GO:0000086	G2/M transition of mitotic cell cycle	0.0261	2.04	GO:0048469	cell maturation	0.0012	4.76
GO:0048313	dendrite morphogenesis	0.0273	3.48	GO:0001224	tol-like receptor signaling pathway	0.0013	2.63
GO:0070585	protein localization to mitochondrion	0.0286	10.74	GO:0035987	endothelial cell differentiation	0.0013	5.55
GO:0006198	cAMP catabolic process	0.0300	5.73	GO:0033138	positive regulation of neptidyl-serine phosphorylation	0.0014	3.37
GO:0010667	negative regulation of cardiac muscle cell	0.0300	5.73	GO:0043536	positive regulation of blood vessel endothelial cell migration	0.0015	6.76
GO:0086005	ventricular cardiac muscle cell action	0.0300	5.73	GO:0009612	response to mechanical stimulus	0.0015	3.63
GO:0007268	chemical synaptic transmission	0.0322	1.70	GO:0032689	negative regulation of interferon-gamma production	0.0016	5.35
GO:0006811	ion transport	0.0346	2.03	GO:0042517	positive regulation of tyrosine phosphorylation of Stat3 protein	0.0017	4.51
GO:0007029	endoplasmic reticulum organization	0.0348	3.98	GO:0060394	negative regulation of pathway-restricted SMAD protein	0.0017	8.92
GO:0010569	regulation of double-strand break repair via	0.0357	5.37	GO:0045669	positive regulation of osteoblast differentiation	0.0017	3.57
GO:0001759	positive regulation of neural precursor cell	0.0357	5.37	GO:0000302	response to reactive oxygen species	0.0019	4.39
GO:0034220	ion transmembrane transport	0.0364	1.74	GO:0002062	chondrocyte differentiation	0.0019	4.39
GO:0000096	positive regulation of Wnt signaling	0.0388	9.20	GO:0050729	positive regulation of inflammatory response	0.0020	3.23
GO:0030913	pancreatic islet assembly	0.0388	9.20	GO:0060325	face morphogenesis	0.0023	5.00
GO:0010882	regulation of cardiac muscle contraction by	0.0388	9.20	GO:0071222	cellular response to lipopolysaccharide	0.0023	2.65
GO:0006887	exocytosis	0.0389	2.33	GO:0002526	acute inflammatory response	0.0024	8.24
GO:0019228	neuronal action potential	0.0391	3.83	GO:0006693	prostaglandin metabolic process	0.0024	8.24
GO:0000145	regulation of cell motility	0.0391	3.83	GO:0042127	regulation of cell proliferation	0.0026	2.20
GO:0032526	response to retinoic acid	0.0404	3.14	GO:0010628	positive regulation of gene expression	0.0028	1.96
GO:1901216	positive regulation of neuron death	0.0419	5.05	GO:0007566	embryo implantation	0.0030	4.68
GO:1903779	regulation of cardiac conduction	0.0449	2.68	GO:0008217	regulation of blood pressure	0.0031	3.30
GO:0007026	chromatin remodeling	0.0465	2.25	GO:0008642	negative regulation of skeletal muscle tissue development	0.0031	12.24
GO:0000338	neurotrophin receptor signaling pathway	0.0465	2.25	GO:0001649	osteoblast differentiation	0.0033	2.68
GO:0007612	learning	0.0483	2.64	GO:0070374	positive regulation of ERK1 and ERK2 cascade	0.0034	2.20
GO:0007413	axonal fasciculation	0.0486	4.77	GO:0046718	viral entry into host cell	0.0039	2.95
GO:0045773	positive regulation of axon extension	0.0487	3.58	GO:0001570	vasculogenesis	0.0042	3.44
GO:0016082	synaptic vesicle priming	0.0502	8.05	GO:0044598	doxorubicin metabolic process	0.0047	10.71
GO:0006661	phosphatidylinositol biosynthetic process	0.0518	2.59	GO:0044597	daunorubicin metabolic process	0.0047	10.71
GO:0035725	sodium ion transmembrane transport	0.0527	2.35	GO:0007265	Ras protein signal transduction	0.0051	3.06
GO:0010976	positive regulation of neuron projection	0.0549	2.17	GO:0051897	positive regulation of protein kinase B signaling	0.0056	2.80
GO:0010765	positive regulation of sodium ion transport	0.0557	4.52	GO:0031100	organ regeneration	0.0058	3.65
GO:0007026	negative regulation of microtubule	0.0557	4.52	GO:0043406	positive regulation of MAP kinase activity	0.0058	3.36
GO:0008045	motor neuron axon guidance	0.0557	4.52	GO:0030097	hemopoiesis	0.0059	3.27
GO:0010881	regulation of cardiac muscle contraction by	0.0557	4.52	GO:0009409	response to cold	0.0059	4.16
GO:1990138	neuron projection extension	0.0557	4.52	GO:0048010	vascular endothelial growth factor receptor signaling pathway	0.0061	2.97
GO:0000266	mitochondrial fission	0.0557	4.52	GO:0048661	positive regulation of smooth muscle cell proliferation	0.0064	3.21
GO:0000122	negative regulation of transcription from	0.0570	1.31	GO:0051603	proteolysis involved in cellular protein catabolic process	0.0065	3.57
GO:0045732	positive regulation of protein catabolic	0.0594	2.51	GO:0006629	lipid metabolic process	0.0067	2.18
GO:0051591	response to cAMP	0.0613	2.80	GO:0032722	positive regulation of chemokine production	0.0069	6.30
GO:0061314	Notch signaling involved in heart	0.0626	7.16	GO:0042448	progesterone metabolic process	0.0069	9.52
GO:0032866	regulation of microtubule-based process	0.0626	7.16	GO:2000737	negative regulation of stem cell differentiation	0.0069	9.52
GO:0035095	behavioral response to nicotine	0.0626	7.16	GO:0001657	ureteric bud development	0.0078	3.95
GO:1903821	regulation of cellular protein localization	0.0626	7.16	GO:0030324	lung development	0.0087	2.82
GO:0006028	regulation of canonical Wnt signaling	0.0634	4.29	GO:0001569	patterning of blood vessels	0.0088	4.59
GO:0045892	negative regulation of transcription, DNA-	0.0637	1.38	GO:0042542	response to hydrogen peroxide	0.0090	3.36
GO:0043647	inositol phosphate metabolic process	0.0661	2.74	GO:0019371	cyclooxygenase pathway	0.0095	8.57
GO:0007264	small GTPase mediated signal transduction	0.0688	1.57	GO:0002675	positive regulation of acute inflammatory response	0.0095	8.57
GO:0008286	insulin receptor signaling pathway	0.0704	2.20	GO:0048662	negative regulation of smooth muscle cell proliferation	0.0102	4.43
GO:0050769	positive regulation of neurogenesis	0.0715	4.09	GO:0035019	somatic stem cell population maintenance	0.0104	2.97
GO:2000727	positive regulation of cardiac muscle cell	0.0759	6.44	GO:0007179	transforming growth factor beta receptor signaling pathway	0.0105	2.56
GO:0046785	microtubule polymerization	0.0759	6.44	GO:0010951	negative regulation of endopeptidase activity	0.0109	2.30
GO:0033148	positive regulation of intracellular estrogen	0.0759	6.44	GO:0042981	regulation of apoptotic process	0.0110	1.91
GO:0042752	regulation of circadian rhythm	0.0763	2.63	GO:0007037	platelet aggregation	0.0112	3.66
GO:0006078	regulation of postsynaptic membrane	0.0800	3.90	GO:0032526	response to retinoic acid	0.0112	3.66
GO:0042059	negative regulation of epidermal growth	0.0845	2.98	GO:0007264	small GTPase mediated signal transduction	0.0115	1.83
GO:0006890	retrograde vesicle-mediated transport,	0.0868	2.09	GO:0007507	heart development	0.0118	1.99
GO:0019722	calcium-mediated signaling	0.0873	2.53	GO:0071395	cellular response to isosmotic acid stimulus	0.0122	16.06
GO:0030335	positive regulation of cell migration	0.0882	1.63	GO:1903553	positive regulation of extracellular exosome assembly	0.0122	16.06
GO:0006469	negative regulation of protein kinase	0.0898	1.95	GO:0010716	negative regulation of extracellular matrix disassembly	0.0122	16.06
GO:0033169	histone H3-K9 demethylation	0.0900	5.86	GO:0070671	response to interleukin-12	0.0122	16.06
GO:0045624	positive regulation of T-helper cell	0.0909	21.47	GO:0000122	negative regulation of transcription from RNA polymerase II	0.0123	1.43
GO:0043490	malate-aspartate shuttle	0.0909	21.47	GO:0046697	decidualization	0.0125	5.35
GO:1909927	calcium ion regulated lysosome exocytosis	0.0909	21.47	GO:0032700	negative regulation of interleukin-17 production	0.0126	7.79
GO:1901205	negative regulation of adrenergic receptor	0.0909	21.47	GO:0051024	positive regulation of immunoglobulin secretion	0.0126	7.79
GO:1904017	cellular response to Thyrolobulin	0.0909	21.47	GO:0051764	actin crosslink formation	0.0126	7.79
GO:0071109	superior temporal gyrus development	0.0909	21.47	GO:0006024	glycosaminoglycan biosynthetic process	0.0126	3.57
GO:0021965	spinal cord ventral commissure	0.0909	21.47	GO:0008203	cholesterol metabolic process	0.0135	2.83
GO:0021549	cerebellum development	0.0914	2.90	GO:0045765	regulation of angiogenesis	0.0135	4.15
GO:0043161	proteasome-mediated ubiquitin-dependent	0.0919	1.59	GO:0030513	positive regulation of BMP signaling pathway	0.0135	4.15
GO:0008344	adult locomotory behavior	0.0931	2.48	GO:0016477	cell migration	0.0148	1.99
GO:0042472	inner ear morphogenesis	0.0931	2.48	GO:0016049	cell growth	0.0148	3.06
GO:0016192	vesicle-mediated transport	0.0974	1.70	GO:0042346	positive regulation of NF-kappaB import into nucleus	0.0149	5.10
GO:0018107	peptidyl-threonine phosphorylation	0.0986	2.83	GO:0071480	cellular response to gamma radiation	0.0149	5.10
GO:0019933	cAMP-mediated signaling	0.0986	2.83	GO:0031954	positive regulation of protein autophosphorylation	0.0149	5.10
GO:0009790	embryo development	0.0986	2.83	GO:0051894	positive regulation of focal adhesion assembly	0.0149	5.10
				GO:0046677	response to antibiotic	0.0154	4.02

GO:0045595	regulation of cell differentiation	0.0154	4.02
GO:0001974	blood vessel remodeling	0.0154	4.02
GO:0007155	cell adhesion	0.0155	1.54
GO:0001934	positive regulation of protein phosphorylation	0.0156	2.19
GO:0002687	positive regulation of leukocyte migration	0.0162	7.14
GO:0050710	negative regulation of cytokine secretion	0.0162	7.14
GO:1990440	positive regulation of transcription from RNA polymerase II	0.0162	7.14
GO:0097067	cellular response to thyroid hormone stimulus	0.0162	7.14
GO:0070301	cellular response to hydrogen peroxide	0.0162	3.01
GO:0032088	negative regulation of NF-kappaB transcription factor activity	0.0172	2.72
GO:0071347	cellular response to interleukin-1	0.0172	2.72
GO:0010718	positive regulation of epithelial to mesenchymal transition	0.0175	3.89
GO:0006928	movement of cell or subcellular component	0.0186	2.49
GO:0001822	kidney development	0.0186	2.49
GO:0003151	outflow tract morphogenesis	0.0193	3.26
GO:0001837	epithelial to mesenchymal transition	0.0197	3.78
GO:0038033	positive regulation of endothelial cell chemotaxis by VEGF-	0.0198	12.85
GO:1990314	cellular response to insulin-like growth factor stimulus	0.0198	12.85
GO:0070306	lens fiber cell differentiation	0.0203	6.59
GO:0001878	response to veast	0.0203	6.59
GO:0051770	positive regulation of nitric-oxide synthase biosynthetic process	0.0203	6.59
GO:0031641	regulation of myelination	0.0203	6.59
GO:0050679	positive regulation of epithelial cell proliferation	0.0211	2.86
GO:0032760	positive regulation of tumor necrosis factor production	0.0212	3.19
GO:0051781	positive regulation of cell division	0.0212	3.19
GO:0045600	positive regulation of fat cell differentiation	0.0212	3.19
GO:0071230	cellular response to amino acid stimulus	0.0212	3.19
GO:0006865	amino acid transport	0.0221	3.67
GO:0050918	positive chemotaxis	0.0221	3.67
GO:0007517	muscle organ development	0.0228	2.41
GO:0034976	response to endoplasmic reticulum stress	0.0232	2.57
GO:0010862	positive regulation of pathway-restricted SMAD protein	0.0234	3.12
GO:0048041	focal adhesion assembly	0.0237	4.46
GO:0043065	positive regulation of apoptotic process	0.0243	1.64
GO:0060395	SMAD protein signal transduction	0.0248	2.76
GO:0032743	positive regulation of interleukin-2 production	0.0250	6.12
GO:0014070	response to organic cyclic compound	0.0256	3.06
GO:0030308	negative regulation of cell growth	0.0258	2.12
GO:0032355	response to estradiol	0.0259	2.35
GO:0071158	positive regulation of cell cycle arrest	0.0272	4.28
GO:0051898	negative regulation of protein kinase B signaling	0.0273	3.47
GO:0042130	negative regulation of T cell proliferation	0.0276	3.47
GO:0006936	muscle contraction	0.0276	2.20
GO:0000187	activation of MAPK activity	0.0276	2.20
GO:0034134	toll-like receptor 2 signaling pathway	0.0287	10.71
GO:0090336	positive regulation of brown fat cell differentiation	0.0287	10.71
GO:0001765	membrane raft assembly	0.0287	10.71
GO:0060754	positive regulation of mast cell chemotaxis	0.0287	10.71
GO:0010742	macrophage derived foam cell differentiation	0.0287	10.71
GO:0060137	maternal process involved in parturition	0.0287	10.71
GO:0006966	alcohol metabolic process	0.0287	10.71
GO:0097084	vascular smooth muscle cell development	0.0287	10.71
GO:0010042	response to manganese ion	0.0287	10.71
GO:2000679	positive regulation of transcription regulatory region DNA	0.0302	5.71
GO:0046688	response to copper ion	0.0302	5.71
GO:0032270	positive regulation of cellular protein metabolic process	0.0302	5.71
GO:0050930	induction of positive chemotaxis	0.0302	5.71
GO:0034446	substrate adhesion-dependent cell spreading	0.0306	3.38
GO:0045930	negative regulation of mitotic cell cycle	0.0310	4.12
GO:0001503	ossification	0.0326	2.41
GO:0034097	response to cytokine	0.0332	2.88
GO:0043410	positive regulation of MAPK cascade	0.0338	2.38
GO:0071456	cellular response to hypoxia	0.0350	2.23
GO:0032728	positive regulation of interferon-beta production	0.0351	3.97
GO:0030949	positive regulation of vascular endothelial growth factor receptor	0.0359	5.35
GO:0003203	endocardial cushion morphogenesis	0.0359	5.35
GO:0048593	camera-type eye morphogenesis	0.0359	5.35
GO:0008283	cell proliferation	0.0366	1.52
GO:0006418	tRNA aminoacylation for protein translation	0.0372	3.21
GO:0045944	positive regulation of transcription from RNA polymerase II	0.0377	1.29
GO:0048146	positive regulation of fibroblast proliferation	0.0390	2.78
GO:0006769	nicotinamide metabolic process	0.0390	9.18
GO:1901385	regulation of voltage-gated calcium channel activity	0.0390	9.18
GO:0048251	elastic fiber assembly	0.0390	9.18
GO:0071455	cellular response to hyperoxia	0.0390	9.18
GO:0034616	response to laminar fluid shear stress	0.0390	9.18
GO:0071679	commissural neuron axon guidance	0.0390	9.18
GO:0043392	negative regulation of DNA binding	0.0395	3.82
GO:0043388	positive regulation of DNA binding	0.0395	3.82
GO:0031589	cell-substrate adhesion	0.0421	5.04
GO:0007219	Notch signaling pathway	0.0423	2.05
GO:0030855	epithelial cell differentiation	0.0441	2.45
GO:0048008	platelet-derived growth factor receptor signaling pathway	0.0441	2.27
GO:0009636	response to toxic substance	0.0444	2.27
GO:0002548	monocyte chemotaxis	0.0446	3.06
GO:0006986	response to unfolded protein	0.0446	3.06
GO:0097191	extrinsic apoptotic signaling pathway	0.0446	3.06
GO:0051496	positive regulation of stress fiber assembly	0.0446	3.06
GO:0008202	steroid metabolic process	0.0486	2.99
GO:0070266	necrototic process	0.0489	4.76
GO:0031668	cellular response to extracellular stimulus	0.0489	4.76
GO:0051017	actin filament bundle assembly	0.0491	3.57
GO:0055072	iron ion homeostasis	0.0491	3.57
GO:0032731	positive regulation of interleukin-1 beta production	0.0504	8.03
GO:0034128	negative regulation of MyD88-independent toll-like receptor	0.0504	8.03
GO:0071236	cellular response to antibiotic	0.0504	8.03
GO:0043129	surfactant homeostasis	0.0504	8.03
GO:0001955	blood vessel maturation	0.0504	8.03
GO:0061180	mammary gland epithelium development	0.0504	8.03
GO:0032825	positive regulation of natural killer cell differentiation	0.0504	8.03
GO:0010888	negative regulation of lipid storage	0.0504	8.03
GO:0002576	platelet degranulation	0.0511	2.08
GO:0070373	negative regulation of ERK1 and ERK2 cascade	0.0524	2.48
GO:0051259	protein oligomerization	0.0524	2.58
GO:0043200	response to amino acid	0.0544	3.45
GO:0006915	apoptotic process	0.0549	1.36
GO:0001701	in utero embryonic development	0.0551	1.72
GO:0010629	negative regulation of gene expression	0.0555	1.88
GO:0046579	positive regulation of Ras protein signal transduction	0.0561	4.51
GO:0060122	inner ear receptor stereocilium organization	0.0561	4.51
GO:0045879	negative regulation of smoothened signaling pathway	0.0561	4.51
GO:0007584	response to nutrient	0.0566	2.32
GO:0032755	positive regulation of interleukin-6 production	0.0572	2.86
GO:0006935	chemotaxis	0.0589	1.93
GO:0050900	leukocyte migration	0.0589	1.93
GO:0050873	brown fat cell differentiation	0.0600	3.35
GO:0042102	positive regulation of T cell proliferation	0.0600	2.50
GO:0043433	negative regulation of sequence-specific DNA binding	0.0600	2.50
GO:0010595	positive regulation of endothelial cell migration	0.0618	2.79
GO:0032729	positive regulation of interferon-gamma production	0.0618	2.79
GO:0048103	somatic stem cell division	0.0629	7.14

GO:0046007	negative regulation of activated T cell proliferation	0.0629	7.14
GO:0090244	Wnt signaling pathway involved in somitogenesis	0.0629	7.14
GO:0035767	endothelial cell chemotaxis	0.0629	7.14
GO:0050807	regulation of synapse organization	0.0629	7.14
GO:0002237	response to molecule of bacterial origin	0.0629	7.14
GO:0006220	pyrimidine nucleotide metabolic process	0.0629	7.14
GO:0035313	wound healing, spreading of epidermal cells	0.0629	7.14
GO:1900119	positive regulation of execution phase of apoptosis	0.0629	7.14
GO:0071243	cellular response to arsenic-containing substance	0.0629	7.14
GO:0030216	keratinocyte differentiation	0.0636	2.25
GO:0060021	palate development	0.0636	2.25
GO:0017015	regulation of transforming growth factor beta receptor signaling	0.0638	4.28
GO:0006541	glutamine metabolic process	0.0638	4.28
GO:0001933	negative regulation of protein phosphorylation	0.0640	2.46
GO:0006508	proteolysis	0.0648	1.37
GO:0009887	organ morphogenesis	0.0651	2.10
GO:0010634	positive regulation of epithelial cell migration	0.0658	3.25
GO:0042110	T cell activation	0.0667	2.73
GO:0051260	protein homooligomerization	0.0709	1.69
GO:0045987	positive regulation of smooth muscle contraction	0.0719	4.08
GO:0045861	negative regulation of proteolysis	0.0719	4.08
GO:0048844	artery morphogenesis	0.0719	4.08
GO:0042730	fibrinolysis	0.0719	4.08
GO:0043330	response to exogenous dsRNA	0.0720	3.15
GO:0050727	regulation of inflammatory response	0.0726	2.38
GO:0043123	positive regulation of I-kappaB kinase/NF-kappaB signaling	0.0738	1.73
GO:0050728	negative regulation of inflammatory response	0.0751	2.17
GO:0003184	pulmonary valve morphogenesis	0.0762	6.43
GO:0051272	positive regulation of cellular component movement	0.0762	6.43
GO:0035999	tetrahydrofolate interconversion	0.0762	6.43
GO:0042359	vitamin D metabolic process	0.0762	6.43
GO:0046888	negative regulation of hormone secretion	0.0762	6.43
GO:0060044	negative regulation of cardiac muscle cell proliferation	0.0762	6.43
GO:0032940	secretion by cell	0.0762	6.43
GO:0010737	protein kinase A signaling	0.0762	6.43
GO:0048048	embryonic eye morphogenesis	0.0762	6.43
GO:0014067	negative regulation of phosphatidylinositol 3-kinase signaling	0.0762	6.43
GO:0033160	positive regulation of protein import into nucleus, translocation	0.0762	6.43
GO:0046653	tetrahydrofolate metabolic process	0.0762	6.43
GO:0071560	cellular response to transforming growth factor beta stimulus	0.0769	2.62
GO:0042632	cholesterol homeostasis	0.0771	2.34
GO:0090090	negative regulation of canonical Wnt signaling pathway	0.0793	1.71
GO:0006090	pyruvate metabolic process	0.0805	3.89
GO:0090023	positive regulation of neutrophil chemotaxis	0.0805	3.89
GO:0034113	heterotypic cell-cell adhesion	0.0805	3.89
GO:0046427	positive regulation of JAK-STAT cascade	0.0805	3.89
GO:0043627	response to estrogen	0.0818	2.31
GO:0051384	response to glucocorticoid	0.0818	2.31
GO:0030593	neutrophil chemotaxis	0.0866	2.27
GO:0035924	cellular response to vascular endothelial growth factor stimulus	0.0895	3.72
GO:0032987	positive regulation of collagen biosynthetic process	0.0895	3.72
GO:0070536	protein K63-linked ubiquitination	0.0895	3.72
GO:0032733	positive regulation of interleukin-10 production	0.0895	3.72
GO:0009617	response to bacterium	0.0895	3.72
GO:0031076	embryonic camera-type eye development	0.0904	5.84
GO:0060445	branching involved in salivary gland morphogenesis	0.0904	5.84
GO:0046849	bone remodeling	0.0904	5.84
GO:0045806	negative regulation of endocytosis	0.0904	5.84
GO:0001946	lymphangiogenesis	0.0904	5.84
GO:0032703	negative regulation of interleukin-2 production	0.0904	5.84
GO:0050927	positive regulation of positive chemotaxis	0.0904	5.84
GO:0048333	mesodermal cell differentiation	0.0904	5.84
GO:0048711	positive regulation of astrocyte differentiation	0.0904	5.84
GO:0032495	response to muramyl dipeptide	0.0904	5.84
GO:0061045	negative regulation of wound healing	0.0904	5.84
GO:0002446	neutrophil mediated immunity	0.0904	5.84
GO:0019049	evasion or tolerance of host defenses by virus	0.0911	21.42
GO:0019322	pentose biosynthetic process	0.0911	21.42
GO:0038190	VEGF-activated neuropilin signaling pathway	0.0911	21.42
GO:1905049	negative regulation of metalloproteinase activity	0.0911	21.42
GO:0090259	regulation of retinal ganglion cell axon guidance	0.0911	21.42
GO:0071418	cellular response to amine stimulus	0.0911	21.42
GO:0046456	icosanoid biosynthetic process	0.0911	21.42
GO:0070427	nucleotide-binding oligomerization domain containing 1 signaling	0.0911	21.42
GO:0003430	growth plate cartilage chondrocyte growth	0.0911	21.42
GO:0015942	formate metabolic process	0.0911	21.42
GO:0015966	diadenosine tetraphosphate biosynthetic process	0.0911	21.42
GO:0060434	bronchus morphogenesis	0.0911	21.42
GO:0006011	UDP-glucose metabolic process	0.0911	21.42
GO:1902336	positive regulation of retinal ganglion cell axon guidance	0.0911	21.42
GO:0009051	pentose-phosphate shunt, oxidative branch	0.0911	21.42
GO:0006919	activation of cysteine-type endopeptidase activity involved in	0.0921	2.06
GO:0051092	positive regulation of NF-kappaB transcription factor activity	0.0926	1.77
GO:0019233	sensory perception of pain	0.0938	2.47
GO:0070371	ERK1 and ERK2 cascade	0.0989	3.57
GO:0048870	cell motility	0.0989	3.57
GO:0032720	negative regulation of tumor necrosis factor production	0.0993	2.82
GO:0010811	positive regulation of cell-substrate adhesion	0.0993	2.82

Supplementary Table S7

S7a) Table of commonly enriched GO terms in iNs and iPSC-iNs. Related to Fig.7.

description	Term	iN_count	iN_pval	iN_fold	iN_benjamini	iPSCiN_count	iPSCiN_pval	iPSCiN_fold	iPSCiN_benjamini
clustering of voltage-gated potassium channels	GO:0045163	2	0.07181945	27.10573043	0.776890918	2	0.063122077	30.92449355	0.910407594
potassium ion export across plasma membrane	GO:0097623	2	0.094596886	20.32929782	0.844569952	2	0.083266989	23.19337017	0.934247631
synaptic vesicle exocytosis	GO:0016079	6	0.000162	11.0887079	0.023283788	3	0.080293574	6.325464591	0.930876438
regulation of potassium ion transmembrane transport	GO:1901379	4	0.005356125	10.84229217	0.229363986	3	0.040237943	9.277348066	0.851969398
ionotropic glutamate receptor signaling pathway	GO:0035235	5	0.002571169	8.470540759	0.154614569	3	0.093320005	5.798342541	0.947842364
glutamate receptor signaling pathway	GO:0007215	3	0.051077622	8.131719128	0.70170925	3	0.040237943	9.277348066	0.851969398
response to nicotine	GO:0035094	7	0.000257	7.692166743	0.028163856	5	0.007929489	6.268478423	0.513265624
positive regulation of calcium ion-dependent exocytosis	GO:0045956	3	0.057449643	7.623486683	0.740422017	4	0.004481464	11.59668508	0.456296747
cation transmembrane transport	GO:0098655	8	0.000157	6.776432607	0.02447448	4	0.083984463	3.865561694	0.932427459
regulation of membrane potential	GO:0042391	12	2.03E-06	6.505375303	0.000959	10	3.19E-05	6.184898711	0.050680544
glutamate secretion	GO:0014047	4	0.030508574	5.808370806	0.567184497	4	0.021688933	6.62667719	0.707990752
potassium ion transmembrane transport	GO:0071805	17	4.39E-08	5.712364677	4.15E-05	11	0.000284	4.216976394	0.206639886
learning	GO:0007612	8	0.000467	5.706469564	0.043225868	6	0.007491992	4.882814772	0.513330264
cardiac conduction	GO:0061337	6	0.004732138	5.421146086	0.215377716	6	0.00269414	6.184898711	0.329191019
locomotory behavior	GO:0007626	11	3.88E-05	5.324339905	0.008119911	9	0.000444	4.970007893	0.134642208
positive regulation of synapse assembly	GO:0051965	8	0.000782	5.246270405	0.065081	5	0.044244598	3.740866156	0.856115543
central nervous system development	GO:0007417	15	1.45E-06	5.082324455	0.000912	7	0.045056254	2.705893186	0.846857405
negative regulation of neuron differentiation	GO:0045665	7	0.002424111	5.082324455	0.151257569	6	0.006954474	4.970007893	0.50839991
potassium ion transport	GO:0006813	10	0.000178	4.958365322	0.023743704	6	0.03174396	3.394151732	0.786598311
memory	GO:0007613	7	0.004059479	4.590486605	0.202567272	5	0.044244598	3.740866156	0.856115543
chemical synaptic transmission	GO:0007268	27	2.37E-10	4.57409201	4.48E-07	13	0.0059056	2.512615101	0.474210594
axonogenesis	GO:0007409	11	0.000145	4.563719919	0.02465333	7	0.019086343	3.313338595	0.673870778
neuron development	GO:0048666	5	0.02592229	4.41941257	0.529004571	4	0.076004336	4.033629594	0.923754709
neurotransmitter secretion	GO:0007269	5	0.036120318	3.986136828	0.624817946	5	0.023761442	4.54771964	0.717174035
neuron migration	GO:0001764	10	0.001112788	3.872247204	0.080810269	10	0.000435	4.417784793	0.162255115
regulation of ion transmembrane transport	GO:0034765	10	0.001645849	3.662936544	0.112960556	10	0.000654	4.178985615	0.141054233
regulation of insulin secretion	GO:0050796	6	0.024208175	3.641068266	0.509982106	6	0.014535116	4.154036448	0.629610882
synapse assembly	GO:0007416	5	0.062537502	3.332671774	0.754485021	7	0.001943012	5.323068563	0.271399742
nervous system development	GO:0007399	23	2.55E-06	3.258354355	0.000964	17	0.000506	2.74764664	0.1283637
axon guidance	GO:0007411	11	0.005930277	2.812858818	0.230264987	12	0.000661	3.500886063	0.125918134
brain development	GO:0007420	11	0.019074577	2.353918695	0.449726518	11	0.008165984	2.685548124	0.504688499
transport	GO:0006810	20	0.001016804	2.336700899	0.080279776	13	0.073810548	1.732838001	0.925771743

S7b) Table of all GO terms enriched in down- and up-regulated genes in iNs versus fibroblasts, and iPSC-iNs versus iPSCs. Related to Fig.7.

Term	Description	Count	Benjamini	Term	Description	Count	Benjamini
iN_down				iN_up			
GO:0051301	cell division	43	2.45E-13	GO:0007268	chemical synaptic transmission	27	4.48E-07
GO:0098609	cell-cell adhesion	29	5.50E-07	GO:0071805	potassium ion transmembrane transport	17	4.15E-05
GO:0007062	sister chromatid cohesion	16	4.66E-05	GO:0007417	central nervous system development	15	9.12E-04
GO:0007067	mitotic nuclear division	24	7.39E-05	GO:0042391	regulation of membrane potential	12	9.59E-04
GO:0051017	actin filament bundle assembly	9	2.97E-04	GO:0007399	nervous system development	23	9.64E-04
GO:0007076	mitotic chromosome condensation	7	4.40E-04	GO:0007218	neuropeptide signaling pathway	13	0.00213378
GO:0006260	DNA replication	15	0.01620475	GO:0021707	cerebellar granule cell differentiation	5	0.00623009
GO:0030048	actin filament-based movement	6	0.01490455	GO:0021549	cerebellum development	8	0.00653324
GO:0007059	chromosome segregation	10	0.01495381	GO:0007626	locomotory behavior	11	0.00811991
GO:0007052	mitotic spindle organization	7	0.02227078	GO:0035725	sodium ion transmembrane transport	10	0.01343861
GO:0001701	in utero embryonic development	16	0.02185359	GO:0007409	axonogenesis	11	0.02465333
GO:0045765	regulation of angiogenesis	7	0.02251181	GO:0098655	cation transmembrane transport	8	0.02447448
GO:0051056	regulation of small GTPase mediated signal transduction	13	0.03186185	GO:0060078	regulation of postsynaptic membrane potential	6	0.02328379
GO:0007229	integrin-mediated signaling pathway	11	0.03777637	GO:0016079	synaptic vesicle exocytosis	6	0.02328379
GO:0008360	regulation of cell shape	13	0.04136013	GO:0006813	potassium ion transport	10	0.0237437
GO:0000082	G1/S transition of mitotic cell cycle	11	0.04209825	GO:0086091	regulation of heart rate by cardiac conduction	7	0.02328449
GO:0000070	mitotic sister chromatid segregation	6	0.04986004	GO:0086012	membrane depolarization during cardiac muscle cell action potential	5	0.02501254
GO:0071897	DNA biosynthetic process	6	0.05686589	GO:0035094	response to nicotine	7	0.02816386
GO:0034616	response to laminar fluid shear stress	4	0.0627906	GO:0007271	synaptic transmission, cholinergic	7	0.02816386
GO:0007179	transforming growth factor beta receptor signaling pathway	10	0.06690727	GO:0017157	regulation of exocytosis	6	0.03844869
GO:0042117	monocyte activation	4	0.08797532	GO:0086005	ventricular cardiac muscle cell action potential	5	0.03841284
GO:0030335	positive regulation of cell migration	14	0.09878239	GO:0007612	learning	8	0.04322587
iPSC_iN_down				GO:2000117	negative regulation of cysteine-type endopeptidase activity	5	0.04528739
GO:0030198	extracellular matrix organization	15	0.20253865	GO:0086002	cardiac muscle cell action potential involved in contraction	5	0.04528739
GO:0030335	positive regulation of cell migration	14	0.19663062	GO:0051965	positive regulation of synapse assembly	8	0.065081
GO:0035019	somatic stem cell population maintenance	8	0.29677418	GO:0006810	transport	20	0.08027978
GO:0016266	O-glycan processing	7	0.6180297	GO:0010765	positive regulation of sodium ion transport	5	0.07826129
GO:0060395	SMAD protein signal transduction	7	0.59803918	GO:0001764	neuron migration	10	0.08081027
GO:0006936	muscle contraction	9	0.55298412	iPSC_iN_up			
GO:0016540	protein autophagy	4	0.50213229	GO:0042391	regulation of membrane potential	10	0.05068054
GO:0003382	epithelial cell morphogenesis	4	0.53433765	GO:0071805	potassium ion transmembrane transport	11	0.20663989
GO:0008284	positive regulation of cell proliferation	21	0.54186876	GO:0000160	phosphorelay signal transduction system	4	0.16099862
GO:1904707	positive regulation of vascular smooth muscle cell proliferation	4	0.52865355	GO:0001764	neuron migration	10	0.16225512
GO:0030168	platelet activation	9	0.49613517	GO:0007626	locomotory behavior	9	0.13464221
GO:0070374	positive regulation of ERK1 and ERK2 cascade	11	0.58579783	GO:0007399	nervous system development	17	0.1283637
GO:2000249	regulation of actin cytoskeleton reorganization	4	0.628204	GO:0034765	regulation of ion transmembrane transport	10	0.14105423
GO:0018108	peptidyl-tyrosine phosphorylation	10	0.61058416	GO:0007411	axon guidance	12	0.12591813
GO:0016337	single organismal cell-cell adhesion	8	0.58918766	GO:0043547	positive regulation of GTPase activity	25	0.20113002
GO:0030154	cell differentiation	20	0.57565884	GO:0007416	synapse assembly	7	0.27139974
GO:0007166	cell surface receptor signaling pathway	14	0.59388133	GO:0061337	cardiac conduction	6	0.32919102
GO:0042060	wound healing	7	0.59035757	GO:0045956	positive regulation of calcium ion-dependent exocytosis	4	0.45629675
GO:0048015	phosphatidylinositol-mediated signaling	8	0.59658965	GO:0002931	response to ischemia	5	0.48299449
GO:0030049	muscle filament sliding	5	0.59486363	GO:0001508	action potential	4	0.46446782
GO:0010837	regulation of keratinocyte proliferation	3	0.67496875	GO:0007268	chemical synaptic transmission	13	0.47421059
GO:0045766	positive regulation of angiogenesis	8	0.69758356	GO:0045665	negative regulation of neuron differentiation	6	0.50839991
GO:0007601	visual perception	11	0.68665858	GO:0007612	learning	6	0.51333026
GO:0010863	positive regulation of phospholipase C activity	3	0.71294909	GO:0035094	response to nicotine	5	0.51326562
GO:0035456	response to interferon-beta	3	0.71294909	GO:0007420	brain development	11	0.50468885
GO:0070588	calcium ion transmembrane transport	8	0.713888	GO:0021516	dorsal spinal cord development	3	0.52137637
GO:0001938	positive regulation of endothelial cell proliferation	6	0.73428974	GO:2000096	positive regulation of Wnt signaling pathway, planar cell polarity pathway	3	0.52137637
GO:0003151	outflow tract morphogenesis	5	0.72631608	GO:0050896	response to stimulus	6	0.56286991
GO:0010595	positive regulation of endothelial cell migration	5	0.72631608	GO:0007379	segment specification	3	0.58595536
GO:0006935	chemotaxis	8	0.71789653	GO:0035556	intracellular signal transduction	17	0.63361299
GO:0050900	leukocyte migration	8	0.71789653	GO:0050796	regulation of insulin secretion	6	0.62961088
GO:0035455	response to interferon-alpha	3	0.7205214	GO:0051291	protein heterooligomerization	6	0.62961088
GO:0070098	chemokine-mediated signaling pathway	6	0.72359054	GO:0018095	protein polyglutamylation	3	0.62662828

Term	Description	Count	Benjamini
GO:0006955	immune response	17	0.78562155
GO:2000648	positive regulation of stem cell proliferation	3	0.80850546
GO:0090399	replicative senescence	3	0.80850546
GO:0007281	germ cell development	4	0.80090288
GO:0045944	positive regulation of transcription from RNA polymerase II promoter	32	0.79969328
GO:0014066	regulation of phosphatidylinositol 3-kinase signaling	6	0.79541355
GO:0006508	proteolysis	19	0.79248787
GO:0051807	defense response to virus	9	0.79154207
GO:0045651	positive regulation of macrophage differentiation	3	0.80311547
GO:0006813	potassium ion transport	6	0.82109396
GO:0043401	steroid hormone mediated signaling pathway	5	0.83014403
GO:0010839	negative regulation of keratinocyte proliferation	3	0.82384074
GO:0050918	positive chemotaxis	4	0.85045141
GO:0072593	reactive oxygen species metabolic process	4	0.85045141
GO:0002042	cell migration involved in sprouting angiogenesis	3	0.84861409
GO:0008585	female gonad development	3	0.84861409
GO:0051260	protein homooligomerization	9	0.84822545
GO:0048661	positive regulation of smooth muscle cell proliferation	5	0.84359874
GO:1902943	positive regulation of voltage-gated chloride channel activity	2	0.83882505
GO:0043407	negative regulation of MAP kinase activity	4	0.83892842
GO:0042981	regulation of apoptotic process	10	0.85114094
GO:0007179	transforming growth factor beta receptor signaling pathway	6	0.87658906
GO:0032331	negative regulation of chondrocyte differentiation	3	0.87190405
GO:0071276	cellular response to cadmium ion	3	0.87190405
GO:1902476	chloride transmembrane transport	6	0.87631013
GO:0043087	regulation of GTPase activity	5	0.87281271
GO:0014068	positive regulation of phosphatidylinositol 3-kinase signaling	5	0.87281271
GO:0046854	phosphatidylinositol phosphorylation	6	0.87628258
GO:0008285	negative regulation of cell proliferation	15	0.8738897
GO:0043280	positive regulation of cysteine-type endopeptidase activity involved in apoptotic process	4	0.86997803
GO:0030225	macrophage differentiation	3	0.87009444
GO:0050870	positive regulation of T cell activation	3	0.87009444
GO:0007597	blood coagulation, intrinsic pathway	3	0.87009444
GO:0051209	release of sequestered calcium ion into cytosol	4	0.87685551
GO:0001842	neural fold formation	2	0.88599365
GO:1900005	positive regulation of serine-type endopeptidase activity	2	0.88599365
GO:2000544	regulation of endothelial cell chemotaxis to fibroblast growth factor	2	0.88599365
GO:1900164	nodal signaling pathway involved in determination of lateral mesoderm left/right asymmetry	2	0.88599365
GO:0060715	syncytiotrophoblast cell differentiation involved in labyrinthine layer development	2	0.88599365
GO:0071294	cellular response to zinc ion	3	0.88247022
GO:0045926	negative regulation of growth	3	0.88247022
GO:0002548	monocyte chemotaxis	4	0.87914417
GO:0010628	positive regulation of gene expression	11	0.88140296
GO:0045785	positive regulation of cell adhesion	4	0.88561642
GO:0035584	calcium-mediated signaling using intracellular calcium source	3	0.88958788
GO:1902895	positive regulation of pri-miRNA transcription from RNA polymerase II promoter	3	0.88958788
GO:0032496	response to lipopolysaccharide	8	0.88857654
GO:0007275	multicellular organism development	18	0.88648318
GO:0016338	calcium-independent cell-cell adhesion via plasma membrane cell-adhesion molecules	3	0.8997086
GO:0007187	G-protein coupled receptor signaling pathway, coupled to cyclic nucleotide second messenger	4	0.90641342
GO:0051091	positive regulation of sequence-specific DNA binding transcription factor activity	6	0.90938391
GO:0010719	negative regulation of epithelial to mesenchymal transition	3	0.90872356
GO:0051781	positive regulation of cell division	4	0.90832045
GO:0061041	regulation of wound healing	2	0.90607647
GO:0051919	positive regulation of fibrinolysis	2	0.90607647
GO:0033634	positive regulation of cell-cell adhesion mediated by integrin	2	0.90607647
GO:0038001	paracrine signaling	2	0.90607647
GO:0031077	post-embryonic camera-type eye development	2	0.90607647
GO:0022617	extracellular matrix disassembly	5	0.90824161
GO:0010862	positive regulation of pathway-restricted SMAD protein phosphorylation	4	0.91031218
GO:0008360	regulation of cell shape	7	0.90994997
GO:0035924	cellular response to vascular endothelial growth factor stimulus	3	0.90806858
GO:0034220	ion transmembrane transport	9	0.91471518
GO:0009615	response to virus	6	0.91660806
GO:0019827	stem cell population maintenance	4	0.9171152

Term	Description	Count	Benjamini
GO:0006836	neurotransmitter transport	4	0.67444446
GO:0048935	peripheral nervous system neuron development	3	0.67573534
GO:0007409	axogenesis	7	0.67387078
GO:0014047	glutamate secretion	4	0.70799075
GO:0030036	actin cytoskeleton organization	8	0.70622907
GO:0007269	neurotransmitter secretion	5	0.71717404
GO:0000187	activation of MAPK activity	7	0.76391651
GO:0007601	visual perception	10	0.77851049
GO:0006813	potassium ion transport	6	0.78659831
GO:1901381	positive regulation of potassium ion transmembrane transport	3	0.8519694
GO:0046928	regulation of neurotransmitter secretion	3	0.8519694
GO:0007215	glutamate receptor signaling pathway	3	0.8519694
GO:1901379	regulation of potassium ion transmembrane transport	3	0.8519694
GO:0007264	small GTPase mediated signal transduction	11	0.8459321
GO:0007423	sensory organ development	2	0.85229569
GO:0007613	memory	5	0.85611554
GO:0051965	positive regulation of synapse assembly	5	0.85611554
GO:2001240	negative regulation of extrinsic apoptotic signaling pathway in absence of ligand	4	0.85176677
GO:0048813	dendrite morphogenesis	4	0.85176677
GO:0007417	central nervous system development	7	0.84685741
GO:0016486	peptide hormone processing	3	0.84160612
GO:0018108	peptidyl-tyrosine phosphorylation	8	0.84856794
GO:0001574	ganglioside biosynthetic process	3	0.88816953
GO:0061763	multivesicular body-lysosome fusion	2	0.91040759
GO:1900452	regulation of long term synaptic depression	2	0.91040759
GO:0033387	putrescine biosynthetic process from ornithine	2	0.91040759
GO:0033605	positive regulation of catecholamine secretion	2	0.91040759
GO:0072102	glomerulus morphogenesis	2	0.91040759
GO:0045163	clustering of voltage-gated potassium channels	2	0.91040759
GO:0030070	insulin processing	2	0.91040759
GO:2000463	positive regulation of excitatory postsynaptic potential	3	0.92143761
GO:0097503	sialylation	3	0.92143761
GO:0035584	calcium-mediated signaling using intracellular calcium source	3	0.92143761
GO:0019226	transmission of nerve impulse	3	0.92143761
GO:0023014	signal transduction by protein phosphorylation	4	0.91847131
GO:0032870	cellular response to hormone stimulus	4	0.92526337
GO:0006810	transport	13	0.92577174
GO:0050772	positive regulation of axonogenesis	3	0.92229185
GO:0048666	neuron development	4	0.92375471
GO:0016079	synaptic vesicle exocytosis	3	0.93087644
GO:0001502	cartilage condensation	3	0.93087644
GO:0039702	viral budding via host ESCRT complex	3	0.93087644
GO:0060999	positive regulation of dendritic spine development	3	0.93087644
GO:0034653	retinoic acid catabolic process	2	0.93424763
GO:0071395	cellular response to jasmonic acid stimulus	2	0.93424763
GO:0097623	potassium ion export across plasma membrane	2	0.93424763
GO:0071205	protein localization to juxtaparanode region of axon	2	0.93424763
GO:0051048	negative regulation of secretion	2	0.93424763
GO:0010701	positive regulation of norepinephrine secretion	2	0.93424763
GO:0098655	cation transmembrane transport	4	0.93242746
GO:0007422	peripheral nervous system development	3	0.94784236
GO:0035235	ionotropic glutamate receptor signaling pathway	3	0.94784236
GO:0000122	negative regulation of transcription from RNA polymerase II promoter	22	0.95206633